Journal of the Turkish Chemical Society Section: A Chemistry

Turkish Chemical Society

The Effects of Thiosemicarbazone-based Oxovanadium (IV) Complex on the Lens and Skin Tissues in Streptozotocin-Induced Diabetic Rats and Computational Studies for the Key Target Proteins of the Lens Tissues

Refiye Yanardag[1*], Onur Ertik[2], Tulay Bal Demirci[3], Bahri Ulkuseven[3], Sevim Tunali[1]

[1]Istanbul University-Cerrahpaşa, Faculty of Engineering, Department of Chemistry, Biochemistry Division, Avcilar, 34320, Istanbul, Türkiye.
[2]Bursa Technical University, Faculty of Engineering and Natural Sciences, Department of Chemistry, Yildirim, 16310, Bursa, Türkiye.
[3]Istanbul University-Cerrahpaşa, Faculty of Engineering, Department of Chemistry, Inorganic Chemistry Division, Avcilar, 34320, Istanbul, Türkiye.

Abstract: A vanadium compound, 2,4-dihydroxybenzylidene-N(4)-2-hydroxybenzylidene-S-methyl-isothiosemicarbazidato-oxidovanadium(IV) (VOL), was investigated for its possible benefits in the treatment of diabetes-related symptoms. Male Swiss albino rats aged 3 to 3.5 months were used in the study. The animals were randomly assigned to four groups. Experimental diabetes was induced by a single intraperitoneal injection of streptozotocin (STZ) at a dose of 65 mg/kg. The groups were as follows: Group I – healthy control (no treatment); Group II – healthy control rats administered VOL; Group III – STZ-induced diabetic rats; Group IV – STZ-induced diabetic rats treated with VOL. After diabetes was induced, VOL was administered to the rats in Groups II and IV via gavage at a daily dose of 0.2 mM/kg for 12 consecutive days. Based on biochemical results, in lens and skin tissues, reduced glutathione levels, catalase, and superoxide dismutase activities were increased, whereas lipid peroxidation and non-enzymatic glycosylated levels were decreased in VOL-treated diabetic rats. Besides that, enzyme activities in the polyol pathway decreased in the lens tissues of diabetic animals given VOL. The binding affinities of these two enzymes (AR and SDH) to VOL were also investigated using molecular docking based on the conformational state. The results revealed that the use of VOL can be effective in preventing or at least retarding the development of some diabetic ocular and dermal complications.

Keywords: Diabetes mellitus, Oxidative stress, Lens tissue, Skin tissue, Vanadium complex.

Submitted: July 5, 2025. **Accepted:** October 13, 2025.

Cite this: Yanardag R, Ertik O, Bal Demirci T, Ulkuseven B, Tunali S. The Effects of Thiosemicarbazone-based Oxovanadium (IV) Complex on the Lens and Skin Tissues in Streptozotocin-Induced Diabetic Rats and Computational Studies for the Key Target Proteins of the Lens Tissues. JOTCSA. 2025;12(4): 221-34.

DOI: https://doi.org/10.18596/jotcsa.1734840

***Corresponding author's E-mail:** yanardag@iuc.edu.tr

1. INTRODUCTION

Diabetes mellitus (DM), a condition characterized by high blood sugar levels, is a growing global health problem, with its prevalence expected to reach 12.2% (783.2 million people) by 2045 (1). It is well established today that DM induces increased oxidative stress in various tissues, affecting several metabolic pathways such as glycolytic, hexosamine, and polyol pathways, and deactivation of the insulin signaling pathway, as well as enhancing the formation of advanced glycation end products (AGE) and activation of protein kinase C (PKC) (2).

Lens and skin are target tissues in DM that are seriously affected by hyperglycemia. Ocular complications such as cataract formation are common in both types of diabetes. High glucose levels in patients induce oxidative stress, which increases protein oxidation and aggregation in lens cells, thereby resulting in a detrimental effect on lens opacity and the development of cataract (3,4). About 30-70% of diabetic patients encounter skin lesions, fungal and bacterial infections, and non-communicable diseases such as lipid necrosis and granuloma annulare (5-7). Since different biochemical processes are occurring in the skin tissue during the diabetic process, a precise molecular etiology for all diabetic dermal conditions has not yet been fully clarified (8). However, it is known that diabetic skin may be one of the first organs to show the first signs of diabetes. In some cases, before diabetes is diagnosed, the wound-healing properties of the skin are insufficient, and high blood sugar levels cause the skin barrier function to deteriorate, making the skin dry (xerosis cutis) and prone to infections (7).

In recent years, numerous studies have focused on the relationship between ultra-trace elements such as copper, iron, zinc, vanadium, and selenium and various diseases, including diabetes (9,10). Among these, vanadium and its various compounds have received special attention as potential therapeutic agents for various conditions, including cancer, atherosclerosis, and diabetes (11). Vanadium compounds are generally divided into three main groups: inorganic vanadium salts (vanadate and vanadyl), peroxovanadium complexes, and organic vanadium compounds. While vanadium can exist in more than one oxidation state, under physiological conditions, the pentavalent form (VO_3^-) predominates in extracellular fluids, whereas the tetravalent form (VO^{2+}) is more prevalent inside cells (12,13). If vanadium remains in the bloodstream for an extended period, it is distributed and stored in various tissues (2). Vanadium species enter the cell through passive diffusion, utilizing various channels such as phosphate or sulfate, or membrane transporters including citrate, lactate, and organic anion transporters (11,14). In this context, vanadium uptake into cells in the form of ligand complexes is increased (15). The hypoglycemic action of vanadium is due to its insulin-mimetic or insulin-enhancing feature. The biochemistry of vanadium compounds involves glucose uptake, through the inhibition of most phosphatases, stimulation of lipogenesis, and inhibition of lipolysis by modulating several key regulators of lipid metabolism, such as enhancing expression of peroxisome proliferator-activated receptor γ (PPARγ) and the activation of AMP-activated protein kinase (AMPK) (16,17). The insulin-mimicking effect of vanadium is primarily due to its inhibitory action, particularly the nonspecific inhibition of protein tyrosine phosphatase 1B (PTP1B). These types of phosphatases are key negative regulators of insulin signaling, and the inhibition of these enzymes may explain why these compounds could potentially act as hypoglycemic agents (18). Since the anti-hyperglycemic effect of different vanadium compounds has recently drawn attention to the impact of vanadium on Alzheimer's disease, also known as type 3 diabetes (19). Vanadium compounds have been shown to effectively enhance glucose uptake in individuals with diabetes mellitus (DM). Experimental studies suggest that vanadium complexes, initially developed as a vanadate analog for DM treatment, may also play a role in regulating amyloid-beta (Aβ) plaque formation associated with Alzheimer's disease (20,21). Additionally, considering the relationship between DM and COVID-19, and in light of their broad biological activity, vanadium compounds are considered promising candidates for future antiviral therapies targeting SARS-CoV-2 infection (17).

In our study, inspired by the insulin-mimetic effects of vanadium and its derivatives in various diabetic models, we aimed to evaluate the therapeutic effect of the VOL complex we synthesized on DM-induced damage to lens and skin tissues by analyzing various biochemical parameters. Additionally, applying molecular docking of VOL to the two target enzymes in the polyol pathway helped us more clearly to investigate the potential role of this compound in DM.

2. EXPERIMENTAL SECTION

2.1. Preparation of Starting Material and Complex VOL

The starting material is 2,4-dihydroxybenzaldehyde-S-methyl-isothiosemicarbazone to obtain the title complex. This compound was prepared using the previously mentioned methods (22-24). S-methyl-isothiosemicarbazide (1 mmol) was dissolved in ethanol (50 mL). 2,4-dihydroxybenzaldehyde (1 mmol) was added to the thiosemicarbazide solution and refluxed for 4 hours. The cream-colored precipitate was filtered and washed with ethanol. The melting point of the product obtained in 88% yield and the melting point was 180-181ºC.

Complex VOL, [2,4-dihydroxybenzylidene-N(4)-2-hydroxybenzylidene-S-methyl-isothiosemicarbazida-tooxidovanadium(IV)], was synthesized from the reaction of the starting material, vanadyl sulfate, and 2-hydroxybenzaldehyde (25). The starting material (1 mmol) and 2-hydroxybenzaldehyde (1 mmol) were dissolved in 50 mL of ethanol. The mixture was added to the $VOSO_4.5H_2O$ (1 mmol) solution in 25 mL of ethanol in a balloon flask, and the homogeneous solution was allowed to stir for 5 hours at room temperature. The brownish-powder product was filtered, and its structure was confirmed by elemental analysis and IR spectrum (Figure 1). Yield 61%, m.p. > 380 °C. μeff: 1.64 BM. Anal. Calc. for $C_{16}H_{13}N_3O_4SV$ (394.3 g mol^{-1}): Found (calc.): C, 48.73 (48.74); H, 3.28 (3.30); N, 10.68 (10.66); S, 8.04 (8.09). UV-Vis (λ nm in DMSO): 245, 315, 352, 418, 800, 958. IR (ATR, cm^{-1}): ν(OH) 3411, ν(C=N) 1605, 1593, 1578, ν(C−O) 1146-1123, ν(V=O) 985, ν(V-O) 477-434.

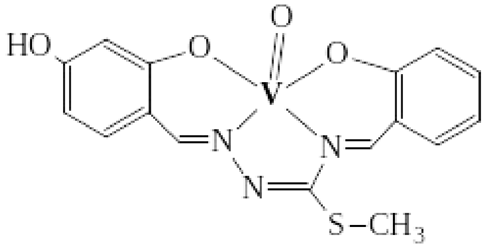

Figure 1: 2,4-dihydroxybenzylidene-N (4)-2-hydroxybenzylidene-S-methyl isothiosemicarbazidato-oxidovanadium (IV), [VOL].

2.2. Experiment Design and Diabetes Induction

All experimental stages in the study were reviewed and approved by the Istanbul University Animal Care and Use Committee. For the experiments, clinically healthy 3.0–3.5-month-old male Swiss Albino rats were used. The experimental animals were randomly assigned to four groups with the following intraperitoneal (i.p.) injection and oral administration protocols: (1) Control (intact) group (n = 5); (2) Control VOL group, receiving VOL via gavage at a dose of 0.2 mmol/kg/day for 12 days (n = 5); (3) STZ-induced diabetic group, made diabetic through intraperitoneal (i.p.) injection of STZ (n = 6); (4) Diabetic group treated with VOL at the same dose and duration (n = 5). Based on the work of Melchior et al., 3% w/w gum arabic was used in the administration of VOL to the animals (25). On the other hand, induction of experimental diabetes was performed with a freshly prepared solution of STZ dissolved in a cold 0.01 M sodium citrate–hydrochloric acid buffer (pH = 4.5) and applied intraperitoneally with a single dose of 65 mg/kg body weight (26). All rats in the experimental groups developed DM. On the 12th day of the experiment, the animals were fasted overnight and euthanized the following day. All collected lens and skin tissues were immediately frozen and stored at -76℃ until the day of analysis. Fasting blood glucose levels after 18 hours were measured using the method described by Relander and Raiha (1963) (27). Data on blood sugar and weight parameters were previously discussed in our research by Yanardag et al. (2009) (24). A cold saline solution (0.9% NaCl) was employed to prepare 10% (w/v) homogenates for both tissues. Following centrifugation (10,000 g, 4°C, 10 min), the resulting clear supernatant was diluted in appropriate ratios and utilized for all biochemical analyses.

2.3. Tissues Non-Enzymatic Oxidative Stress Parameters and Protein Content

The reduced glutathione (GSH) content was measured using the Beutler’s method, employing the Ellman reagent (1975) (28). The process measures the SH group reduction capacity, which forms a yellow color with Ellman’s reagent to obtain 5,5′-dithiobis (2-nitrobenzoic acid). Measurements were performed spectrophotometrically at 412 nm, and the results were expressed as nmol GSH/mg protein.

Ledwozyw’s method (1986) was used for lipid peroxidation (LPO) assays (29). Briefly, tissue homogenates treated with thiobarbituric acid are boiled and extracted with *n*-butanol. The obtained colored extracts are measured spectrophotometrically, and the results are expressed as nmol MDA/mg protein.

Thiobarbituric acid method was used to determine lens and skin non-enzymatic glycosylated (NEG) levels (30). Incubating the tissue homogenates with oxalic acid converts the glucose moieties of glycosylated tissue proteins to 5-hydroxymethyl furfural, which is yellow when 2-thiobarbituric acid is added to the reaction medium. The Lowry method was used to measure the tissue homogenates' protein levels, and the results were expressed as nmol fructose/mg protein (31). The activities of the antioxidant enzymes catalase (CAT) and superoxide dismutase (SOD) in lens and skin tissue were determined using the methods of Aebi (1984) (32) and Mylroie et al. (1986) (33).

2.4. Lens Tissue Polyol Pathway Enzymes

Hayman and Kinoshita’s (1965) method was used to determine the activity of lens aldose reductase (AR) in the lens tissue (34). After adding phosphate buffer, NADPH, and lens supernatant solutions at appropriate rates, the reaction mixture was started in a sample cuvette by adding DL-glyceraldehyde as a substrate. The final volume was obtained as 1 mL with a pH of 6.2. A double-beam spectrophotometer was used to record absorbance (ΔA) changes at 340 nm for 3 min at 30-second intervals. AR activity was expressed as ΔA/min/g protein. The activity of sorbitol dehydrogenase (SDH) was measured using the method described by Barretto and Beutler (1975) (35). The reaction mixture was prepared by adding 1 M Tris (pH 8.0), 50 mM NAD^+, 100 mM $MgCl_2$, and diluted lens tissue homogenate. The final volume was made 1 mL with the addition of distilled water. After incubating the mixture at 37 °C for 10 minutes, the reaction was initiated by adding a 200 mM sorbitol solution. The increase in absorbance was recorded at 340 nm for 4 minutes at 60-second intervals, and enzyme activity was expressed as U/g protein.

2.5. Analysis of the Results

The unpaired t-test and analysis of variance (ANOVA) were used to analyze the biochemical results, which were calculated using the NCSS statistical software package. Results were expressed as mean ± SD, with $p < 0.05$ considered statistically significant.

2.6. Computational Studies

Theoretical calculations for the investigated VOL were performed using the Gaussian 09 program package, applying the density functional theory (DFT) method with the hybrid B3LYP functional and the LANL2DZ basis set (36). For this purpose, the three-dimensional structure of the VOL complex was first drawn using the Avagadro program and then saved in mol2 format. Next, the DFT-based B3LYP method with the standard LANL2DZ basis set was employed to optimize the geometry of the VOL fully. The representations and contributions of the highest occupied molecular orbital (HOMO) and the lowest unoccupied molecular orbital (LUMO) were also calculated. The orbital density distributions of HOMO and LUMO, as well as the molecular electrostatic potential (MEP), were visualized and plotted using GaussView 5.0.

2.7. Computational Studies

A molecular docking process was performed for AR and SDH, which are target enzymes in diabetes and lens tissue. Two steps were made for this preparation: i) preparation of proteins and ii) preparation of ligands. In the preparation of proteins, the three-dimensional structures of AR (PDB ID: 1IEI) and SDH (PDB ID: 1PL6) were downloaded from the Protein Data Bank site as PDB files. Molecules other than water and amino acids were deleted, polar hydrogens were added and saved in PDB format to make docking ready (37,38). The structure of the VOL was optimized based on the B3LYP/LANL2D theory using Gaussian 09, and the most stable structure was chosen for docking calculations. In order to understand the inhibitory effect of Complex VOL on target proteins, inhibitor molecules found in AR and SDH structures (Zenarestat - PubChem CID: 5724 and 4-[2-(hydroxymethyl)pyrimidin-4-yl]-N, N-dimethyl piperazine-1-sulfonamide - PubChem CID: 132302, respectively) were re-docked, and it was aimed to compare VOL with standard molecules. For this purpose, standard molecules downloaded from the PubChem site were re-docked by energy minimization using Universal Force Field (UFF) (39). After preparation of proteins and ligands, docking for target proteins was performed using the AMDock program with Autodock 4.2 (40). For AR, X: -6.8, Y: -1.4, Z: 9.3, and for SDH, X: -94.3, Y: 38.3, Z: 33.9, a grid box was determined, and the grid size was entered as 25x25x25—the 3D and 2D interaction of ligands and protein was monitored by using Dassault Systèmes Discovery Studio, 2021.

2.8. The Root Mean Square Fluctuation (RMSF) Analysis

Following the identification of the protein-ligand interaction, the stability of the protein-ligand complex was assessed in this work using the CABS-fex 2.0 server and displayed using RMSF (http://biocomp.chem.uw.edu.pl/CABSflex2/index) (41,42).

3. RESULTS AND DISCUSSION

3.1. Synthesis, UV-Vis, and IR spectroscopy

Complex VOL was obtained from the thiosemicarbazone and aldehyde by the template effect of oxovanadium (II) ion. We monitored the formation of the complex with IR spectrum. The disappearance of bands attributed to the 2-OH and NH_2 groups observed in the starting material and the emergence of bands related to the V=O and V-O vibrations were evidences of the formation of the structure of VOL (25). The imine groups of the starting material were observed at 1608 and 1585 cm^{-1}, and the hydroxyl group at 3495 cm^{-1}. Infrared spectrum of VOL showed bands at 1605, 1593, 1578 cm^{-1} attributed to C=N1 and N4=C bands, and in the spectrum of VOL, the stretching and bending bands at 3445, 3337, and 1624 cm^{-1} of amine group disappeared while new bands at 985, 477-434 cm^{-1} assigned to V=O and V-O groups were observed. The UV-Vis spectrum of the VOL complex showed the charge transfer bands at 245, 315, and 352 nm assigned to $\pi\rightarrow\pi^*$ and $n\rightarrow\pi^*$, d-d bands at 418, 800, and 958 nm (25).

The structure and purity of VOL were verified by elemental analysis and thin-layer chromatography (TLC) for the biological tests. The stability of VOL in the gum Arabic solution (the biological medium used in this study) and in a polar solvent (a 1:1 water-DMSO mixture) was investigated by monitoring its UV-Vis spectrum. The absorption and λmax values remained unchanged over a period of 20 days.

3.2. VOL Effect on Body Weight and Fasting Blood Glucose Levels of the Experimental Rats

Fasting blood sugar and weight values of the animals used in the study were published in our previous research (24). Here, the weight loss observed in diabetic rats was significantly prevented by VOL treatment administered on days 1, 6, and 12. Similarly, it was found that the increase in blood glucose levels caused by STZ administration was reduced through oral VOL treatment (24).

3.3. VOL Effect on Non-Enzymatic Oxidative Stress Parameters Content in the Lens and Skin Tissues of the Experimental Rats

GSH level in diabetic lens tissues was significantly reduced ($p < 0.001$) compared to control rats (Table 1). Significant differences in skin GSH levels were also found among the diabetic and control groups ($p < 0.001$) (Table 2). VOL application to the hyperglycemic rats resulted in a mean increase in the GSH level of both lens and skin tissues in comparison to STZ-induced animals ($p < 0.0001$; $p < 0.0001$) (Table 1; Table 2).

The LPO levels in the lens and skin tissues of the diabetic groups were significantly higher than those of the non-treated control rats ($p < 0.05$; $p < 0.0001$) (Table 1; Table 2). After vanadyl complex administration to diabetic animals, tissue LPO levels significantly decreased as compared to untreated diabetic animals ($p < 0.05$; $p < 0.05$) (Table 1; Table 2).

Table 1: Lens tissue GSH, LPO, and NEG levels for all groups*.

Group	GSH (nmol GSH/mg protein)	LPO (nmol MDA/mg protein	NEG (nmol Fructose/mgprotein)
Control	12.0 ± 1.8	0.5 ± 0.2	6.8 ± 0.5
Control + VOL	7.0 ± 1.0	0.6 ± 0.1	8.8 ± 1.4
Diabetic	4.6 ± 0.4[a]	0.8 ± 0.2[c]	49.0 ± 3.8[e]
Diabetic + VOL	8.7 ± 1.1[b]	0.4 ± 0.2[d]	30.8 ± 7.4[f]
P_{ANOVA}	0.0001	0.005	0.0001

*Mean ± SD
[a]p < 0.001 vs control
[b]p < 0.0001vs diabetic group
[c]p < 0.05 vs control
[d]p < 0.05 vs diabetic group
[e]p < 0.0001 vs control
[f]p < 0.001 vs diabetic group

Table 2: Skin tissue GSH, LPO, and NEG levels for all groups*.

Group	GSH (nmol GSH/mg protein)	LPO (nmol MDA/mg protein)	NEG (nmol Fructose/ mg protein)
Control	19.5 ± 1.1	1.4 ± 0.6	19.2 ± 2.3
Control + VOL	47.1 ± 7.8	1.6 ± 0.1	24.6 ± 2.0
Diabetic	12.2 ± 2.5[a]	2.1 ± 0.1[a]	35.5 ± 3.7[d]
Diabetic + VOL	34.4 ± 1.7[b]	1.5 ± 0.2[c]	21.7 ± 3.4[e]
P_{ANOVA}	0.0001	0.076	0.0001

*Mean ± SD
[a]p < 0.05 versus control
[b]p < 0.0001 versus diabetic group
[c]p < 0.05 versus diabetic group
[d]p < 0.0001 versus control
[e]p < 0.001 versus diabetic group

A significant increase in the NEG levels was observed in both tissues of diabetic rats in comparison of control group animals ($p < 0.0001$; $p < 0.0001$), whereas in the diabetic group given VOL, this parameter in the same tissues declined significantly in comparison to hyperglycemic group, respectively ($p < 0.001$; $p < 0.001$) (Table 1; Table 2).

3.4. VOL Effects on Enzymatic Oxidative Stress Parameters in the Lens and Skin Tissues of Experimental Rats

The activities of CAT in the diabetic lens and skin tissues are lower than those of non-diabetic rats; the differences were statistically significant ($p < 0.001$; $p < 0.0001$) (Table 3; Table 4). After VOL treatment in diabetic rats, catalase (CAT) activity in both tissues showed a statistically significant increase compared to untreated diabetic animals ($p < 0.005$; $p < 0.0001$) (Table 3; Table 4). On the other hand, lens and skin SOD activities were significantly reduced in the diabetic group compared to the non-treated animals ($p < 0.05$; $p < 0.05$) (Table 3; Table 4). Treatment with VOL for 12 days caused an elevation of the SOD activities in diabetic lens and skin tissues ($p < 0.05$; $p < 0.05$) (Table 3; Table 4).

Table 3: Lens tissue CAT and SOD activities for all groups *.

Group	CAT (U/mg protein)	SOD (U/mg protein)
Control	101.3 ± 3.8	1.6 ± 0.1
Control + VOL	106.3 ± 7.8	0.7 ± 0.3
Diabetic	85.8 ± 3.6[a]	1.4 ± 0.1[c]
Diabetic + VOL	93.7 ± 3.1[b]	2.3 ± 0.1[d]
P_{ANOVA}	0.0001	0.001

*Mean ± SD
[a]p < 0.001 versus control
[b]p < 0.005 versus diabetic group
[c]p < 0.05 versus control
[d]p < 0.05 versus diabetic group

Table 4: Skin tissue CAT and SOD activities for all groups*.

Group	CAT (U/mg protein)	SOD (U/mg protein)
Control	2.3 ± 0.5	5.1 ± 0.8
Control + VOL	0.8 ± 0.1	5.9 ± 0.4
Diabetic	0.5 ± 0.1[a]	3.4 ± 0.1[c]
Diabetic + VOL	0.8 ± 0.1[b]	4.6 ± 0.5[d]
P_{ANOVA}	0.0001	0.006

*Mean ± SD
[a]$p < 0.0001$ versus control
[b]$p < 0.0001$ versus diabetic group
[c]$p < 0.05$ versus control group
[d]$p < 0.05$ versus diabetic group

3.5. VOL Effect on Polyol Pathway Enzymes in the Lens Tissue of the Experimental Rats

There was a significant increase in the activities of the enzymes AR and SDH in the lens tissue of the diabetic rats in comparison with the control non-treated rats ($p < 0.0001$; $p < 0.002$). In the diabetic animals given VOL, the polyol pathway enzyme activities were significantly restored in comparison with the diabetic group without any treatment ($p < 0.0001$; $p < 0.003$) (Table 5).

Table 5: Lens tissue AR and SDH activities for all groups*.

Group	AR (U/g protein)	SDH (U/g protein)
Control	2.9 ± 0.5	0.7 ± 0.1
Control + VOL	4.3 ± 0.7	1.3 ± 0.6
Diabetic	8.1 ± 1.4[a]	14.1 ± 0.9[c]
Diabetic + VOL	2.3 ± 0.8[b]	1.6 ± 0.1[d]
P_{ANOVA}	0.0001	0.020

*Mean ± SD
[a]$p < 0.0001$ versus control
[b]$p < 0.0001$ versus diabetic group
[c]$p < 0.002$ versus control
[d]$p < 0.003$ versus diabetic group

3.6. Computational Studies

A small Eg ($Eg = E_{LUMO} - E_{HOMO}$) value reflects the reactivity of the complexes, which leads to softness. In contrast, a wide energy gap between HOMO and LUMO complicates electron transfer, resulting in hard compounds (43). The HOMO and LUMO values calculated for VOL were found to be -0.15045 and -0.10921 eV, respectively, and the Eg value was calculated as 0.04124 eV (Figure 2A). The molecular electrostatic potential (MEP) contributes to understanding molecular reactivity, charge distribution, and the locations of electrophilic and nucleophilic assaults in the molecule (44). The red hue represents the largest negative area chosen for electrophilic attack, whereas the blue color represents the positive region preferred for nucleophilic reaction for the VOL (Figure 2B).

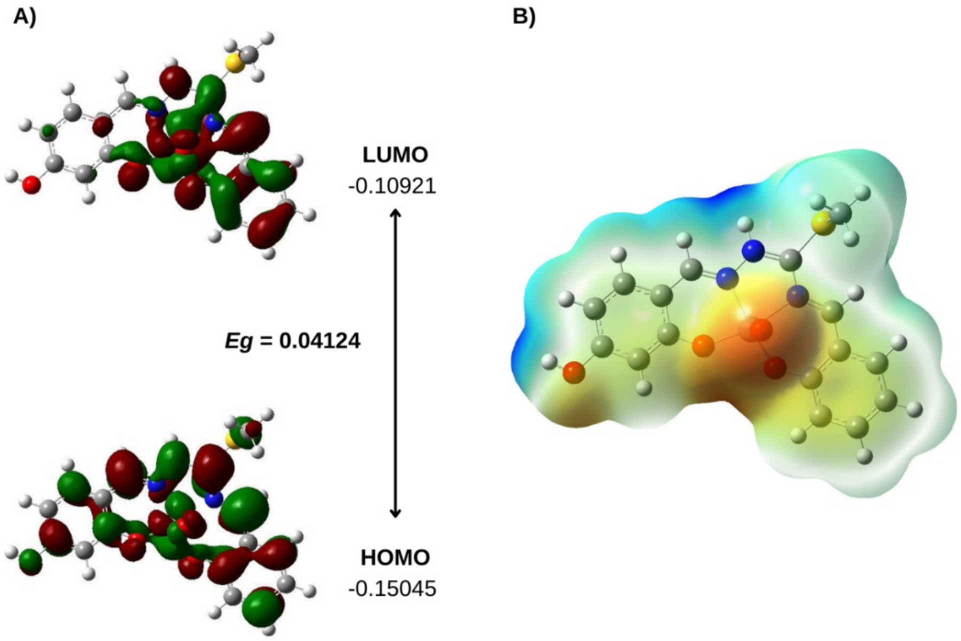

Figure 2: A) HOMO-LUMO representation and B) molecular electrostatic potential (MEP) analysis of the VOL.

3.7. Molecular Docking Studies

In the *in-vivo* studies, molecular docking was applied to understand whether VOL has potential inhibitory properties for AR and SDH, parameters whose activities decrease when VOL treatment is used, and the binding scores of each target protein are given in Table 6. It was found that the standard molecule Zenarestat (-10.17 kcal/mol) and VOL (-10.04 kcal/mol) had close binding affinities for AR, while for SDH, it was found to have higher binding affinities than the standard molecule (-6.18 kcal/mol) (-7.54 kcal/mol).

Table 6: Molecular docking results of the VOL and standards to the target proteins (AR and SDH).

	AR		SDH	
Compounds	**Docking Scores** (kcal/mol)	**Estimated K_i** (nM)	**Docking Scores** (kcal/mol)	**Estimated K_i** (nM)
VOL	-10.04	43.72	-7.54	2.97
Zenarestat	-10.17	35.10	-	-
4-[2-(hydroxymethyl)pyrimidin-4-yl]-N,N-dimethylpiperazine-1-sulfonamide	-	-	-6.18	29.51

The 3D and 2D protein-ligand interactions of the interactions of target proteins with VOL and standard molecules are presented in Figure 3. For AR, VAL47, TYR48, TRP111, and CYS298, residues are seen to be molecules that interact in common for both VOL and the standard molecules. However, differences in the interaction with VOL and the standard molecule were detected for TRP111 and CYS298 residues. While hydrogen bonds were observed between these residues and the standard molecule, these interactions were found to be hydrophobic interactions for VOL. When detailed protein-ligand interactions were examined for SDH, it was seen that the interactions were different except for ILE183 and ARG298 residues. While VOL had hydrophobic interactions for ILE183 and ARG298 residues, it was found that the standard molecule formed hydrophobic bonds with ILE183 and hydrogen bonds with ARG298. It can be suggested that these hydrophobic interactions of VOL may have affected the stability of the protein-ligand complexes and resulted in better docking results.

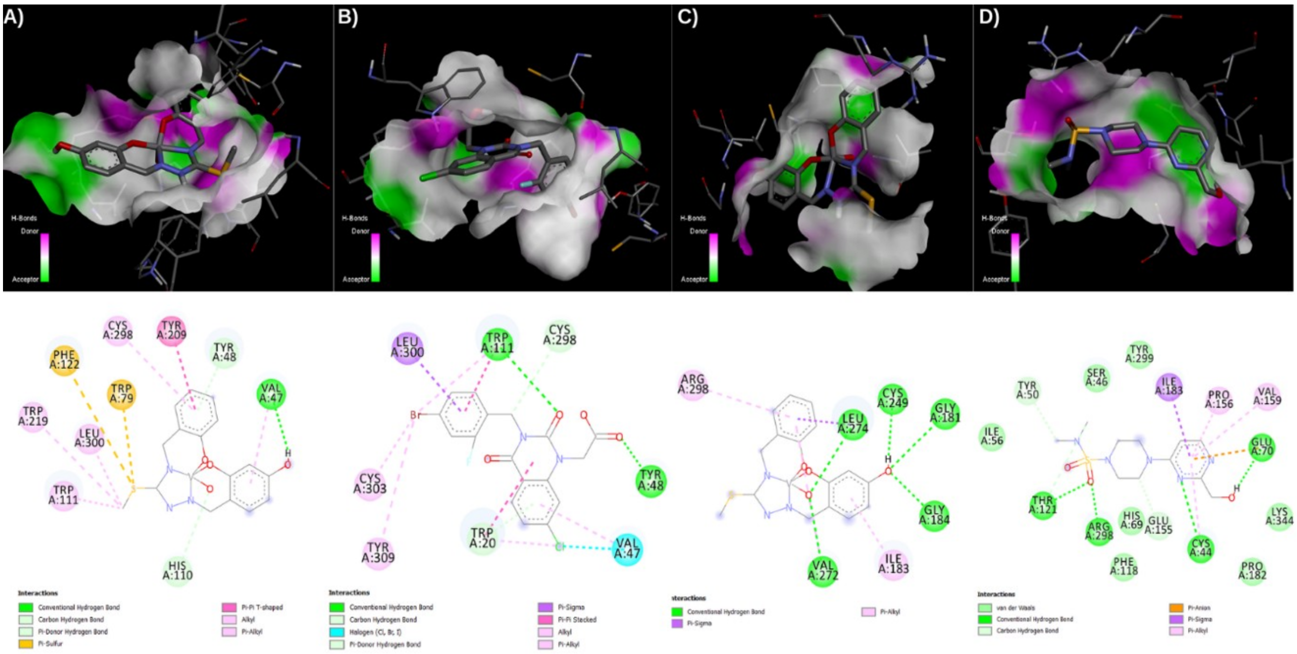

Figure 3: The 3D and 2D protein-ligand interactions with the target proteins. A) AR-VOL, B) AR-standard, C) SDH-VOL, D) SDH-standard complexes, respectively.

3.8. The Root Mean Square Fluctuation (RMSF) Analysis

RMSF, in terms of protein-ligand interactions, represents the average deviation or volatility of individual atoms in a molecule from their mean location over time.

RMSF is frequently employed in protein-ligand interactions to investigate the flexibility or dynamic behavior of a protein and its ligand complex during molecular dynamics simulations. RMSF offers information on whether parts of the protein or ligand are more flexible or stiff during the simulation. High RMSF values imply more flexibility, whilst low values indicate higher stiffness. This allows for a better understanding of the interactions between ligands and proteins (45).

The RMSF analysis graph and multimodal superimposed simulated structure of AR and ligand complexes are shown in Figure 4. It was observed that VOL increased the RMSF values in some regions and decreased them in other areas. When the RMSF averages were taken for AR, AR-VOL, and AR-STD, it was determined that they were 0.793±0.554, 0.841±0.656, and 0.838±0.573 Å, respectively.

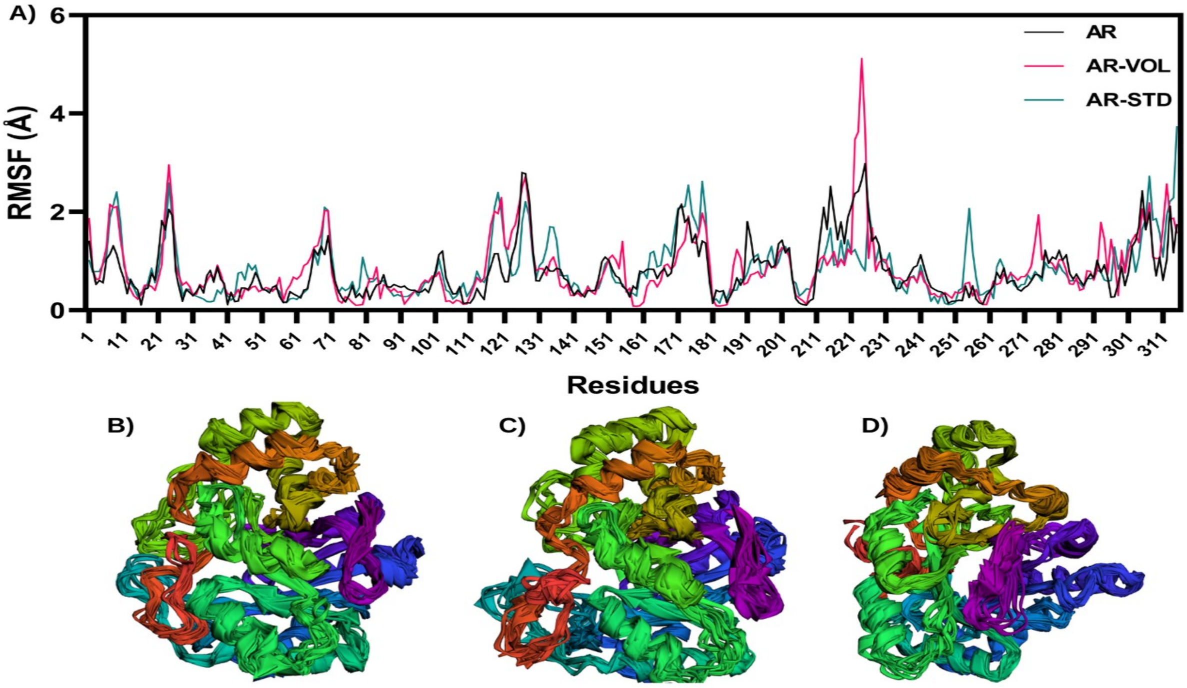

Figure 4: (A) The RMSF analysis of the protein-ligand complexes for AR and multimodel superimposed simulated structure of (B) AR, (C) AR-VOL, (D) AR-STD.

Diabetes mellitus (DM) is a chronic metabolic disorder marked by high blood glucose levels, which occur due to either insulin resistance or impaired insulin secretion. Failure of diabetic therapy to regulate abnormal glycemic control may enhance the risk of macrovascular and microvascular complications, such as diabetic foot, skin tissue, and retinopathy (46-48). Oxidative stress, occurring in the hyperglycemic organism, affects all systems with different mechanisms (49-52).

Studies have indicated that oxidative stress is a crucial factor in the development and progression of diabetes, contributing to pancreatic beta-cell dysfunction, insulin resistance, and various diabetic complications. Therefore, targeting oxidative stress has emerged as a promising therapeutic strategy for managing diabetes and its complications (48).

However, the proposed mechanism for vanadium compounds as an insulin mimic agent is that they enhance the activity of protein kinases in the insulin signal cascade. Also, several studies showed that some vanadium compounds protected beta cells by enhancing phosphorylation of a series of proteins in STZ-induced diabetic mice (53-58). A notable aspect during glucose regulation in the body is the recovery of glycogen synthesis, increased glucose uptake, and improved utilization. This has been observed in studies conducted on type 1 diabetes models treated with vanadium. It has been reported that significant increases in GLUT-4 expression result in improved insulin signaling pathways, leading to increased muscle and cardiac glycogen (59). These effects have led to an expansion in the use of metallotherapeutics today.

In the present study, besides the decreased GSH level, we observed increased LPO and advanced glycosylated end products (AGEs) content in the diabetic animals' lens and skin tissues. The increased polyol pathway enzyme activities and ROS production were also observed in the lens tissue. The decrease in GSH level in the diabetic lens and skin tissues increases the susceptibility to oxidative stress and the detoxification of H_2O_2 (60). The rise in MDA levels and NEG content in the studied two tissues of hyperglycemic animals, as compared to the control group, indicates both enhanced lipid peroxidation and protein oxidation (46,61). The elevated production of lipid peroxides in diabetes compromises the structural integrity of the lens tissue membrane, resulting in the inhibition of various membrane-bound enzymes. Additionally, lipid peroxidation is thought to contribute to the dysfunction of endothelial cells, changes in keratinocyte capillary permeability, and disturbances in fibroblast and collagen metabolism in skin tissue (62).

NEG is one of the post-translational modifications that negatively affect the structure and functions of proteins by cross-linking and aggregation in DM. In the hyperglycemic state, NEG also activates abnormal cellular signaling and transcription factors, as well as modifies gene expression profiles. AGEs are metabolic products that accumulate as a result of the NEG reaction (63). These effects of diabetes have drawn attention towards antioxidants and special metal-chelating compounds having anti-glycation activities, such as the administration of the VOL complex, which has cellular antioxidant properties. Besides that, our findings also support previous research on diabetic lenses and skin tissues (46,47,64-67).

The high production of ROS plays a key role in the initiation and progression of diabetic retinopathy and chronic hyperglycemia. The activation of secondary pathways triggered by hyperglycemic conditions leads to the formation of more ROS species, as well as to the reduction of antioxidant enzymes, thus further increasing damage (68-70). CAT and SOD, the main endogenous antioxidant enzymes, are responsible for protecting tissues from oxidative damage. They convert superoxide ions into hydrogen peroxide and then hydrogen peroxide to non-toxic peroxide compounds (71). More clearly, SOD converts the superoxide anion into H_2O_2 and O_2, while CAT detoxifies H_2O_2 (72). The increased production of H_2O_2 and O_2^-, resulting from the auto-oxidation caused by elevated glucose levels in the organism and the non-enzymatic glycation of proteins, leads to a decrease in the activities of the CAT and SOD enzymes (73,74). These enzyme activities can be partially inactivated by hydroxyl radicals and H_2O_2, as reported previously by Hodgson et al. (1975) and Pigeolet et al. (1990) (75,76). The reduced activities of SOD and CAT may result from the increased production of H_2O_2 and O_2^-, which occurs due to the auto-oxidation of excess glucose and the non-enzymatic glycation of proteins (77). We determined this from the significant increase in the activities of progression oxidative stress marker enzymes in diabetic lens and skin tissues treated with VOL. The ameliorated antioxidant defense system, in both tissues studied in our research, has been considered to be via the antioxidant capacity of oxovanadium complex. In fact, vanadium complexes are promising compounds due to their antidiabetic properties, as well as their antioxidant effect (78-80). Reports by Pranczk (2015) indicate that oxovanadium (IV) complex with iminodiacetate was found to scavenge superoxide free radicals (O_2^{-}) and organic radicals such as $ABTS^+$ and $DPPH^+$ (81). We observed a significant increase in the activities of progression oxidative stress marker enzymes in the lens and skin tissues of diabetic animals treated with VOL. Therefore, controlling the balance between oxidants/antioxidant status can be an effective strategy for attenuating the damage caused by diabetic retinopathy and dermopathy.

The polyol pathway has a major role in the development of opacity in the diabetic rat lenses (82). Increased AR activity under hyperglycemic conditions results in a reduction of NADPH rate, leading to a significant decrease in GSH concentration. The cellular antioxidant capacity is diminished by AR activity during hyperglycemia. The concurrent high activity of the SDH enzyme (excessive conversion of sorbitol to fructose) is among the causes of oxidative stress in lens tissue. Since the co-factor NAD^+ is reduced to NADH in this reaction, NADH causes the formation of ROS species, which are also considered as a starting molecule of NADH oxidase (83). The fructose produced from glucose in this pathway generates two metabolites (fructose-3-phosphate and 3-deoxyglucosone), which are more powerful non-enzymatic glycation agents than glucose. Therefore, the increased AGE formation is a result of glucose flux through the polyol pathway (1). The glucose flux-induced polyol pathway also causes tissue damage via sorbitol-induced osmotic stress. These osmotic changes also lead to degeneration of hydrophobic lens fibers, collapse and liquefaction of lens fibers, and consequently lens opacities and formation of diabetic cataracts (84,85). In the present study, we noted an increase in AR and SDH activities in hyperglycemic lens tissues. The decreased activities of these enzymes were observed upon treatment with vanadyl complex. This may be due to vanadium's insulin mimetic behavior, which provided a controlled normoglycemic state in the diabetic animals, and also the effective restoration of AR and SDH in the lens tissue (55,67).

As a result of *in vivo studies obtained for lens tissue, it was observed that AR and SDH target proteins increased in the diabetes group,* and VOL treatment reversed this increase, suggesting that VOL may be an inhibitor molecule for these target proteins. Therefore, computer-aided analyses, which have been included in studies in recent years, were performed to understand this situation. The binding affinities of VOL and target proteins were compared with molecular docking, and high binding affinities were found for both target proteins. In addition, DFT analyses made structural analysis possible for VOL. As a result, it was revealed that VOL is a potential inhibitor candidate for AR and SDH, which are target proteins for lens tissue in diabetes, especially in understanding the *in vivo* effects.

4. CONCLUSION

Diabetes is a complicated metabolic disorder that contributes to the progression of oxidative stress. In the study, we observed that oxidative stress caused deterioration of the physiology of the lens and skin tissues. Complex VOL conspicuously restored the integrity of lens and skin tissues via antioxidant and antihyperglycemic properties. It improved the tissues' metabolism by reducing oxidative stress in addition to DM therapy—the study gave promising results that require further research on DM therapy, both *in vivo* and *in silico*. By study, VOL is now an ingredient candidate for antidiabetic formulations. Moreover, it has been seen that the investigation of such thiosemicarbazone-based vanadium compounds is an important strategy in the development of drugs.

5. CONFLICT OF INTEREST

The authors declare that they have no conflict of interest.

6. ACKNOWLEDGMENTS

Research Fund of Istanbul University financed this study (Project No: BYP/3864 and Project No: BYP/37135).

7. REFERENCES

1. Geng X, Li Z, Yang Y. Emerging role of epitranscriptomics in diabetes mellitus and its complications. Front Endocrinol (Lausanne) [Internet]. 2022 May 27;13:907060. Available from:

<URL>.

2. Darenskaya MA, Kolesnikova LI, Kolesnikov SI. Oxidative stress: Pathogenetic role in diabetes mellitus and its complications and therapeutic approaches to correction. Bull Exp Biol Med [Internet]. 2021 May 26;171(2):179–89. Available from: <URL>.

3. Gong W, Zhu G, Li J, Yang X. LncRNA MALAT1 promotes the apoptosis and oxidative stress of human lens epithelial cells via p38MAPK pathway in diabetic cataract. Diabetes Res Clin Pract [Internet]. 2018 Oct;144:314–21. Available from: <URL>.

4. Jain AK, Lim G, Langford M, Jain SK. Effect of high-glucose levels on protein oxidation in cultured lens cells, and in crystalline and albumin solution and its inhibition by vitamin B6 and N-acetylcysteine: Its possible relevance to cataract formation in diabetes. Free Radic Biol Med [Internet]. 2002 Dec;33(12):1615–21. Available from: <URL>.

5. Wan X, Gen F, Sheng Y, Ou M, Wang F, Peng T, et al. Meta-analysis of the effect of kangfuxin liquid on diabetic patients with skin ulcers. Chung YC, editor. Evidence-Based Complement Altern Med [Internet]. 2021 Jun 3;2021:1334255. Available from: <URL>.

6. Cheng B, Jiang Y, Fu X, Hao D, Liu H, Liu Y, et al. Epidemiological characteristics and clinical analyses of chronic cutaneous wounds of inpatients in China: Prevention and control. Wound Repair Regen [Internet]. 2020 Sep 25;28(5):623–30. Available from: <URL>.

7. Andrade TAM, Masson-Meyers DS, Caetano GF, Terra VA, Ovidio PP, Jordão-Júnior AA, et al. Skin changes in streptozotocin-induced diabetic rats. Biochem Biophys Res Commun [Internet]. 2017 Sep;490(4):1154–61. Available from: <URL>.

8. Makrantonaki E, Jiang D, Hossini AM, Nikolakis G, Wlaschek M, Scharffetter-Kochanek K, et al. Diabetes mellitus and the skin. Rev Endocr Metab Disord [Internet]. 2016 Sep 19;17(3):269–82. Available from: <URL>.

9. MW Hasanato R. Trace elements in type 2 diabetes mellitus and their association with glycemic control. Afr Health Sci [Internet]. 2020 Apr 20;20(1):287–93. Available from: <URL>.

10. Cancarini A, Fostinelli J, Napoli L, Gilberti ME, Apostoli P, Semeraro F. Trace elements and diabetes: Assessment of levels in tears and serum. Exp Eye Res [Internet]. 2017 Jan;154:47–52. Available from: <URL>.

11. Treviño S, Díaz A, Sánchez-Lara E, Sanchez-Gaytan BL, Perez-Aguilar JM, González-Vergara E. Vanadium in biological action: Chemical, pharmacological aspects, and metabolic implications in diabetes mellitus. Biol Trace Elem Res [Internet]. 2019 Mar 22;188(1):68–98. Available from: <URL>.

12. Tripathi D, Mani V, Pal RP. Vanadium in biosphere and its role in biological processes. Biol Trace Elem Res [Internet]. 2018 Nov 9;186(1):52–67. Available from: <URL>.

13. Harland BF, Harden-Williams BA. Is vanadium of human nutritional importance yet? J Am Diet Assoc [Internet]. 1994 Aug;94(8):891–4. Available from: <URL>.

14. Ścibior A, Pietrzyk Ł, Plewa Z, Skiba A. Vanadium: Risks and possible benefits in the light of a comprehensive overview of its pharmacotoxicological mechanisms and multi-applications with a summary of further research trends. J Trace Elem Med Biol [Internet]. 2020 Sep;61:126508. Available from: <URL>.

15. Lima LMA, Belian MF, Silva WE, Postal K, Kostenkova K, Crans DC, et al. Vanadium(IV)-diamine complex with hypoglycemic activity and a reduction in testicular atrophy. J Inorg Biochem [Internet]. 2021 Mar;216:111312. Available from: <URL>.

16. Irving E, Stoker A. Vanadium compounds as PTP inhibitors. Molecules [Internet]. 2017 Dec 19;22(12):2269. Available from: <URL>.

17. Semiz S. Vanadium as potential therapeutic agent for COVID-19: A focus on its antiviral, antiinflamatory, and antihyperglycemic effects. J Trace Elem Med Biol [Internet]. 2022 Jan;69:126887. Available from: <URL>.

18. Uprety B, Abrahamse H. Targeting breast cancer and their stem cell population through AMPK activation: Novel insights. Cells [Internet]. 2022 Feb 7;11(3):576. Available from: <URL>.

19. He Z, You G, Liu Q, Li N. Alzheimer's disease and diabetes mellitus in comparison: The therapeutic efficacy of the vanadium compound. Int J Mol Sci [Internet]. 2021 Nov 3;22(21):11931. Available from: <URL>.

20. He Z, Li X, Han S, Ren B, Hu X, Li N, et al. Bis(ethylmaltolato)oxidovanadium (IV) attenuates amyloid-beta-mediated neuroinflammation by inhibiting NF-κB signaling pathway via a PPARγ-dependent mechanism. Metallomics [Internet]. 2021 Jul 2;13(7):mfab036. Available from: <URL>.

21. He Z, Han S, Zhu H, Hu X, Li X, Hou C, et al. The protective effect of vanadium on cognitive impairment and the neuropathology of alzheimer's disease in APPSwe/PS1dE9 Mice. Front Mol Neurosci [Internet]. 2020 Mar 10;13:00021. Available from: <URL>.

22. Bal T, Atasever B, Solakoğlu Z, Erdem-Kuruca S, Ülküseven B. Synthesis, characterisation and cytotoxic properties of the N1,N4-diarylidene-S-methyl-thiosemicarbazone chelates with Fe(III) and Ni(II). Eur J Med Chem [Internet]. 2007 Feb;42(2):161–7. Available from: <URL>.

23. Atasever B, Ülküseven B, Bal-Demirci T, Erdem-Kuruca S, Solakoğlu Z. Cytotoxic activities of new iron(III) and nickel(II) chelates of some S-methyl-thiosemicarbazones on K562 and ECV304 cells. Invest New Drugs [Internet]. 2010 Aug 4;28(4):421–32. Available from: <URL>.

24. Yanardag R, Demirci TB, Ülküseven B, Bolkent S, Tunali S, Bolkent S. Synthesis, characterization and

antidiabetic properties of N1-2,4-dihydroxybenzylidene-N4-2-hydroxybenzylidene-S-methyl-thiosemicarbazidato-oxovanadium(IV). Eur J Med Chem [Internet]. 2009 Feb;44(2):818–26. Available from: <URL>.

25. Melchior M, Rettig SJ, Liboiron BD, Thompson KH, Yuen VG, McNeill JH, et al. Insulin-enhancing vanadium(III) complexes. Inorg Chem [Internet]. 2001 Aug 27;40(18):4686–90. Available from: <URL>.

26. Junod A, Lambert AE, Stauffacher W, Renold AE. Diabetogenic action of streptozotocin: Relationship of dose to metabolic response. J Clin Invest [Internet]. 1969 Nov 1;48(11):2129–39. Available from: <URL>.

27. Relander A, Räihä CE. Differences between the enzymatic and O-Toluidine methods of blood glucose determination. Scand J Clin Lab Invest [Internet]. 1963 Jan 13;15(3):221–4. Available from: <URL>.

28. Beutler E. In: Bergmeyen HV, Ed., Red blood cell metabolism: a manual of biochemical methods, 2nd edition, Grune and Stratton, New York. 1975;112–4.

29. Ledwoż;yw A, Michalak J, Stępień A, Kądziołka A. The relationship between plasma triglycerides, cholesterol, total lipids and lipid peroxidation products during human atherosclerosis. Clin Chim Acta [Internet]. 1986 Mar;155(3):275–83. Available from: <URL>.

30. Parker KM, England JD, Da Costa J, Hess RL, Goldstein DE. Improved colorimetric assay for glycosylated hemoglobin. Clin Chem [Internet]. 1981 May 1;27(5):669–72. Available from: <URL>.

31. Lowry OH, Rosebrough NJ, Farr AL, Randall RJ. Protein measurement with the folin phenol reagent. J Biol Chem [Internet]. 1951;193(1):265–75. Available from: <URL>.

32. Aebi H. Catalase in vitro. In 1984. p. 121–6. Available from: <URL>.

33. Mylroie AA, Collins H, Umbles C, Kyle J. Erythrocyte superoxide dismutase activity and other parameters of copper status in rats ingesting lead acetate. Toxicol Appl Pharmacol [Internet]. 1986 Mar;82(3):512–20. Available from: <URL>.

34. Hayman S, Kinoshita JH. Isolation and properties of lens aldose reductase. J Biol Chem [Internet]. 1965 Feb;240(2):877–82. Available from: <URL>.

35. Barretto OCO, Beutler E. The sorbitol-oxidizing enzyme of red blood cells. J Lab Clin Med [Internet]. 1975 Apr 1;85(4):645–9. Available from: <URL>.

36. Frisch M, Trucks G, Schlegel HB, Scuseria GE, Robb MA, Cheeseman JR, et al. Gaussian 09, Revision d. 01; Gaussian, Inc.: Wallingford CT, USA. 2009.

37. Kinoshita T, Miyake H, Fujii T, Takakura S, Goto T. The structure of human recombinant aldose reductase complexed with the potent inhibitor zenarestat. Acta Crystallogr Sect D Biol Crystallogr [Internet]. 2002 Apr 1;58(4):622–6. Available from: <URL>.

38. Pauly TA, Ekstrom JL, Beebe DA, Chrunyk B, Cunningham D, Griffor M, et al. X-ray crystallographic and kinetic studies of human sorbitol dehydrogenase. Structure [Internet]. 2003 Sep;11(9):1071–85. Available from: <URL>.

39. Rappe AK, Casewit CJ, Colwell KS, Goddard WA, Skiff WM. UFF, a full periodic table force field for molecular mechanics and molecular dynamics simulations. J Am Chem Soc [Internet]. 1992 Dec 1;114(25):10024–35. Available from: <URL>.

40. Valdés-Tresanco MS, Valdés-Tresanco ME, Valiente PA, Moreno E. AMDock: A versatile graphical tool for assisting molecular docking with autodock vina and autodock4. Biol Direct [Internet]. 2020 Dec 16;15(1):12. Available from: <URL>.

41. Jamroz M, Kolinski A, Kmiecik S. CABS-flex: Server for fast simulation of protein structure fluctuations. Nucleic Acids Res [Internet]. 2013 Jul 1;41(W1):W427–31. Available from: <URL>.

42. Kmiecik S, Gront D, Kolinski M, Wieteska L, Dawid AE, Kolinski A. Coarse-grained protein models and their applications. Chem Rev [Internet]. 2016 Jul 27;116(14):7898–936. Available from: <URL>.

43. Gunasekaran S, Arun Balaji R, Kumaresan S, Anand G, Srini-Vasan S. Experimental and theoretical investigations of spectroscopic properties of N-acetyl-5-methoxytryptamine. Can J Anal Sci Spectrosc [Internet]. 2008;53(4):149–62. Available from: <URL>.

44. Buvaneswari M, Santhakumari R, Usha C, Jayasree R, Sagadevan S. Synthesis, growth, structural, spectroscopic, optical, thermal, DFT, HOMO–LUMO, MEP, NBO analysis and thermodynamic properties of vanillin isonicotinic hydrazide single crystal. J Mol Struct [Internet]. 2021 Nov 5;1243:130856. Available from: <URL>.

45. Sharma J, Kumar Bhardwaj V, Singh R, Rajendran V, Purohit R, Kumar S. An in-silico evaluation of different bioactive molecules of tea for their inhibition potency against non structural protein-15 of SARS-CoV-2. Food Chem [Internet]. 2021 Jun;346:128933. Available from: <URL>.

46. Tunali S, Yanardag R. Protective effect of vanadyl sulfate on skin injury in streptozotocin-induced diabetic rats. Hum Exp Toxicol [Internet]. 2013 Nov 26;32(11):1206–12. Available from: <URL>.

47. Tunalı S, Yanardağ R. The effects of vanadyl sulfate on glutathione, lipid peroxidation and nonenzymatic glycosylation levels in various tissues in experimental diabetes. İstanbul J Pharm [Internet]. 2021 Apr 30;51(1):73–8. Available from: <URL>.

48. Zhang P, Li T, Wu X, Nice EC, Huang C, Zhang Y. Oxidative stress and diabetes: antioxidative strategies. Front Med [Internet]. 2020 Oct 4;14(5):583–600. Available from: <URL>.

49. Kurt O, Ozden TY, Ozsoy N, Tunali S, Can A, Akev N, et al. Influence of vanadium supplementation on oxidative stress factors in the muscle of STZ-diabetic rats. BioMetals [Internet]. 2011 Oct 10;24(5):943–9. Available from: <URL>.

50. Tunali S, Gezginci-Oktayoglu S, Bolkent S, Coskun E, Bal-Demirci T, Ulkuseven B, et al. Protective effects of an oxovanadium(IV) complex with N_2O_2 chelating thiosemicarbazone on small intestine injury of STZ-diabetic rats. Biol Trace Elem Res [Internet]. 2021 Apr 9;199(4):1515–23. Available from: <URL>.

51. Akgün-Dar K, Bolkent S, Yanardag R, Tunalı S. Vanadyl sulfate protects against streptozotocin-induced morphological and biochemical changes in rat aorta. Cell Biochem Funct [Internet]. 2007 Nov 7;25(6):603–9. Available from: <URL>.

52. Tunali S, Yanardag R. Effect of vanadyl sulfate on the status of lipid parameters and on stomach and spleen tissues of streptozotocin-induced diabetic rats. Pharmacol Res [Internet]. 2006 Mar;53(3):271–7. Available from: <URL>.

53. Fantus IG, George R, Tang S, Chong P, Poznansky MJ. The insulin-mimetic agent vanadate promotes receptor endocytosis and inhibits intracellular Ligand-receptor degradation by a mechanism distinct from the lysosomotropic agents. Diabetes [Internet]. 1996 Aug 1;45(8):1084–93. Available from: <URL>.

54. Gao Z, Zhang C, Yu S, Yang X, Wang K. Vanadyl bisacetylacetonate protects β cells from palmitate-induced cell death through the unfolded protein response pathway. JBIC J Biol Inorg Chem [Internet]. 2011 Jun 22;16(5):789–98. Available from: <URL>.

55. Bolkent S, Bolkent S, Yanardag R, Tunali S. Protective effect of vanadyl sulfate on the pancreas of streptozotocin-induced diabetic rats. Diabetes Res Clin Pract [Internet]. 2005 Nov;70(2):103–9. Available from: <URL>.

56. Cam MC, Li WM, McNeill JH. Partial preservation of pancreatic β-cells by vanadian: Evidence for long-term amelioration of diabetes. Metabolism [Internet]. 1997 Jul;46(7):769–78. Available from: <URL>.

57. Pirmoradi L, Noorafshan A, Safaee A, Dehghani GA. Quantitative assessment of proliferative effects of oral vanadium on pancreatic islet volumes and beta cell numbers of diabetic rats. Iran Biomed J [Internet]. 2016;20(1):18–25. Available from: <URL>.

58. Mohammadi MT, Pirmoradi L, Mesbah F, Safaee A, Dehghani GA. Trophic Actions of Oral Vanadium and Improved Glycemia on the Pancreatic Beta-Cell Ultrastructure of Streptozotocin-Induced Diabetic Rats. J Pancreas [Internet]. 2014;15(6):591–6. Available from: <URL>.

59. Hiromura M, Nakayama A, Adachi Y, Doi M, Sakurai H. Action mechanism of bis(allixinato)oxovanadium(IV) as a novel potent insulin-mimetic complex: Regulation of GLUT4 translocation and FoxO1 transcription factor. JBIC J Biol Inorg Chem [Internet]. 2007 Oct 15;12(8):1275–87. Available from: <URL>.

60. Kahya MC, Nazıroğlu M. Melatonin reduces lens oxidative stress level in STZ-induced diabetic rats through supporting glutathione peroxidase and reduced glutathione values. J Cell Neurosci Oxidative Stress [Internet]. 2016 Dec 31;8(2):588–94. Available from: <URL>.

61. Sun L, Shi DJ, Gao XC, Mi SY, Yu Y, Han Q. The protective effect of vanadium against diabetic cataracts in diabetic rat model. Biol Trace Elem Res [Internet]. 2014 May 8;158(2):219–23. Available from: <URL>.

62. Altavilla D, Saitta A, Cucinotta D, Galeano M, Deodato B, Colonna M, et al. Inhibition of lipid peroxidation restores impaired vascular endothelial growth factor expression and stimulates wound healing and angiogenesis in the genetically diabetic mouse. Diabetes [Internet]. 2001 Mar 1;50(3):667–74. Available from: <URL>.

63. Kumar Pasupulati A, Chitra PS, Reddy GB. Advanced glycation end products mediated cellular and molecular events in the pathology of diabetic nephropathy. Biomol Concepts [Internet]. 2016 Dec 1;7(5–6):293–309. Available from: <URL>.

64. Tarwadi K V., Agte V V. Effect of micronutrients on methylglyoxal-mediated in vitro glycation of albumin. Biol Trace Elem Res [Internet]. 2011 Nov 17;143(2):717–25. Available from: <URL>.

65. Elosta A, Ghous T, Ahmed N. Natural products as anti-glycation agents: Possible therapeutic potential for diabetic complications. Curr Diabetes Rev [Internet]. 2012 Mar 1;8(2):92–108. Available from: <URL>.

66. Wu CH, Yen GC. Inhibitory effect of naturally occurring flavonoids on the formation of advanced glycation endproducts. J Agric Food Chem [Internet]. 2005 Apr 1;53(8):3167–73. Available from: <URL>.

67. Preet A, Gupta BL, Yadava PK, Baquer NZ. Efficacy of lower doses of vanadium in restoring altered glucose metabolism and antioxidant status in diabetic rat lenses. J Biosci [Internet]. 2005 Mar 1;30(2):221–30. Available from: <URL>.

68. Zhang L, Chu W, Zheng L, Li J, Ren Y, Xue L, et al. Zinc oxide nanoparticles from *Cyperus rotundus* attenuates diabetic retinopathy by inhibiting NLRP3 inflammasome activation in STZ-induced diabetic rats. J Biochem Mol Toxicol [Internet]. 2020 Dec 21;34(12):e22583. Available from: <URL>.

69. Giacco F, Brownlee M. Oxidative stress and diabetic complications. Schmidt AM, editor. Circ Res [Internet]. 2010 Oct 29;107(9):1058–70. Available from: <URL>.

70. Lu L, Lu Q, Chen W, Li J, Li C, Zheng Z. Vitamin D $_3$ protects against diabetic retinopathy by inhibiting high-glucose-induced activation of the ROS/TXNIP/NLRP3 inflammasome pathway. J Diabetes Res [Internet]. 2018 Feb 22;2018:8193523. Available from: <URL>.

71. Gong X, Zhang Q, Tan S. Inhibitory effect of r-hirudin variant III on streptozotocin-induced diabetic cataracts in rats. Galuppo M, Xi ZX, editors. Sci World J [Internet]. 2013 Jan 10;2013(1):630651. Available from: <URL>.

72. Zych M, Wojnar W, Kielanowska M, Folwarczna J, Kaczmarczyk-Sedlak I. Effect of berberine on glycation, aldose reductase activity, and oxidative stress in the lenses of streptozotocin-induced diabetic rats in vivo—A preliminary study. Int J Mol Sci [Internet]. 2020 Jun 16;21(12):4278. Available from: <URL>.

73. Siddiqui MR, Taha A, Moorthy K, Hussain ME, Basir SF, Baquer NZ. Amelioration of altered antioxidant status and membrane linked functions by vanadium andTrigonella in alloxan diabetic rat brains. J Biosci [Internet]. 2005 Sep 1;30(4):483–90. Available from: <URL>.

74. Aragno M, Brignardello E, Tamagno E, Gatto V, Danni O, Boccuzzi G. Dehydroepiandrosterone administration prevents the oxidative damage induced by acute hyperglycemia in rats. J Endocrinol [Internet]. 1997 Nov 1;155(2):233–40. Available from: <URL>.

75. Hodgson EK, Fridovich I. Interaction of bovine erythrocyte superoxide dismutase with hydrogen peroxide. Inactivation of the enzyme. Biochemistry [Internet]. 1975 Dec 1;14(24):5294–9. Available from: <URL>.

76. Pigeolet E, Corbisier P, Houbion A, Lambert D, Michiels C, Raes M, et al. Glutathione peroxidase, superoxide dismutase, and catalase inactivation by peroxides and oxygen derived free radicals. Mech Ageing Dev [Internet]. 1990 Feb;51(3):283–97. Available from: <URL>.

77. Sindhu RK, Koo J, Roberts CK, Vaziri ND. Dysregulation of hepatic superoxide dismutase, catalase and glutathione peroxidase in diabetes: response to insulin and antioxidant therapies. Clin Exp Hypertens [Internet]. 2004 Jan 29;26(1):43–53. Available from: <URL>.

78. Du J, Feng B, Dong Y, Zhao M, Yang X. Vanadium coordination compounds loaded on graphene quantum dots (GQDs) exhibit improved pharmaceutical properties and enhanced anti-diabetic effects. Nanoscale [Internet]. 2020;12(16):9219–30. Available from: <URL>.

79. Hadjiadamou I, Vlasiou M, Spanou S, Simos Y, Papanastasiou G, Kontargiris E, et al. Synthesis of vitamin E and aliphatic lipid vanadium(IV) and (V) complexes, and their cytotoxic properties. J Inorg Biochem [Internet]. 2020 Jul;208:111074. Available from: <URL>.

80. del Río D, Galindo A, Vicente R, Mealli C, Ienco A, Masi D. Synthesis, molecular structure and properties of oxo-vanadium(iv) complexes containing the oxydiacetate ligand. Dalt Trans [Internet]. 2003 Apr 17;(9):1813–20. Available from: <URL>.

81. Pranczk J, Jacewicz D, Wyrzykowski D, Wojtczak A, Tesmar A, Chmurzyński L. Crystal structure, antioxidant properties and characteristics in aqueous solutions of the oxidovanadium(IV) Complex [VO(IDA)phen]·$2H_2O$. Eur J Inorg Chem [Internet]. 2015 Jul 22;2015(20):3343–9. Available from: <URL>.

82. Smith DM, Sale GJ. Evidence that a novel serine kinase catalyses phosphorylation of the insulin receptor in an insulin-dependent and tyrosine kinase-dependent manner. Biochem J [Internet]. 1988 Dec 15;256(3):903–9. Available from: <URL>.

83. Morré DM, Lenaz G, Morré DJ. Surface oxidase and oxidative stress propagation in aging. J Exp Biol [Internet]. 2000 May 15;203(10):1513–21. Available from: <URL>.

84. Shibata M, Oshitari T, Kajita F, Baba T, Sato E, Yamamoto S. Development of macular holes after rhegmatogenous retinal detachment repair in japanese patients. J Ophthalmol [Internet]. 2012;2012:740591. Available from: <URL>.

85. Pradeep SR, Srinivasan K. Ameliorative influence of dietary fenugreek (*Trigonella foenum-graecum*) seeds and onion (*Allium cepa*) on eye lens abnormalities via modulation of crystallin proteins and polyol pathway in experimental diabetes. Curr Eye Res [Internet]. 2018 Sep 2;43(9):1108–18. Available from: <URL>.